



## Fission track radiography of uranium and thorium in radioactive minerals

Wollenberg, H.

*Publication date:*  
1971

*Document Version*  
Publisher's PDF, also known as Version of record

[Link back to DTU Orbit](#)

*Citation (APA):*  
Wollenberg, H. (1971). *Fission track radiography of uranium and thorium in radioactive minerals*. Risø National Laboratory. Denmark. Forskningscenter Risø. Risø-R No. 228

---

### General rights

Copyright and moral rights for the publications made accessible in the public portal are retained by the authors and/or other copyright owners and it is a condition of accessing publications that users recognise and abide by the legal requirements associated with these rights.

- Users may download and print one copy of any publication from the public portal for the purpose of private study or research.
- You may not further distribute the material or use it for any profit-making activity or commercial gain
- You may freely distribute the URL identifying the publication in the public portal

If you believe that this document breaches copyright please contact us providing details, and we will remove access to the work immediately and investigate your claim.

Danish Atomic Energy Commission  
Research Establishment Risø

---

# Fission Track Radiography of Uranium and Thorium in Radioactive Minerals

by Harold Wollenberg

July 1971

*Sales distributors:* Jul. Gjellerup, 87, Sølvgade, DK-1307 Copenhagen K, Denmark

*Available on exchange from:* Library, Danish Atomic Energy Commission, Risø, DK-4000 Roskilde, Denmark





Fission Track Radiography of Uranium and Thorium  
in Radioactive Minerals

by

Harold Wollenberg

Danish Atomic Energy Commission  
Research Establishment Risø  
Electronics Department\*

Abstract

The fission track method is a quick, relatively simple, and inexpensive technique to determine the location and abundance of uranium, and in some cases thorium, in thin or polished sections of rocks. Thermal neutrons induce fission in  $^{235}\text{U}$ , while  $^{232}\text{Th}$  and  $^{238}\text{U}$  fission with fast-neutron bombardment. Therefore, sections with appropriate track detectors are exposed first to thermal neutrons to induce only U, then to fast neutrons for U plus Th. The detectors are etched to reveal the damaged areas (tracks) caused by passage of massively charged fission fragments. High quality muscovite mica is the preferable track detector for minerals with U contents greater than 10 to 15 ppm, mainly because tracks in mica are easy to recognize. Polycarbonate plastic (lexan or makrofol) is preferred as a track detector for low contents of U and Th because this material contains essentially no inherent U; therefore it has no background track density. Thorium is determined successfully if the Th/U ratio of the mineral is sufficiently large. Relative errors (from counting statistics) in Th are less than 25% if Th/U is greater than 3, for ratios less than 3 the errors increase rapidly and exceed 40 to 50% if Th/U is less than 1.

\*Work accomplished while on leave from the Lawrence Radiation Laboratory, University of California, Berkeley 94720.

The method was applied to the study of U and Th in rocks of the Ilfmaussaq intrusion, South Greenland, and in a mineralized fault zone occurrence in East Greenland. At Ilfmaussaq the most intense U and Th mineralization is associated with lujavrites of the Kvanefjeld area, where the mineral steenstrupine controls whole-rock radioactivity. Arithmetic mean values of Th and U in steenstrupine are 23000 and 6200 ppm, respectively. In lujavrites of the Kangerdluarssuk area, rock radioactivity is controlled by eudialyte, whose Th and U contents are at least an order of magnitude less than those in steenstrupine. Thorium and uranium contents of monazite, thorite, and pigmentary material were also investigated. Fission track examinations of thin sections of mineralized fault zone breccia from the East Greenland occurrence indicated that U is strongly associated with limonitic material in thin fluoritized veinlets, and is occasionally found concentrated near the edges of reddish opaque (hematite?) grains. By combining fission track results with an electron microprobe study of the minerals one may be able to correlate the abundance of Th and U with other elements.

## CONTENTS

	Page
1. Introduction .....	5
2. The Fission Track Method .....	6
3. Procedures .....	7
3.1. Choice of Detectors .....	8
3.2. Standards .....	10
3.3. Irradiation .....	10
3.4. Etching .....	10
3.5. Observation .....	11
3.6. Thorium Determination .....	11
4. Results and Discussion .....	11
4.1. Radioactive Minerals of the Ilímaussaq Intrusion .....	12
4.1.1. Steenstrupine .....	13
4.1.2. Eudialyte .....	19
4.1.3. Pigmentary Material .....	20
4.1.4. Thorite .....	20
4.1.5. Monazite .....	20
4.2. Comparison with $\alpha$ -Autoradiographic Data .....	24
4.3. An East Greenland Fault Zone Occurrence .....	25
5. Summary and Conclusions .....	28
6. Acknowledgements .....	29
7. Appendix 1 A Scheme for Preparation, Exposure, and Observation of a Thin-Section-Track-Detector Series .....	30
8. Appendix 2 Description of Thin Sections, by Professor Henning Sørensen .....	35
9. References .....	39





## 1. INTRODUCTION

Determination of the location of radioactive minerals in rock thin sections has been accomplished for many years by alpha-track autoradiography. Briefly described,  $\alpha$  particles radiating from U- and Th-bearing zones near the surface of a thin section are registered on an overlying photographic emulsion, which when developed, locates sites of radioactivity and permits quantitative determination of their  $\alpha$ -particle activity (Bowie, 1954; Hamilton, 1960, Buchwald and Sørensen, 1961). A drawback of the technique is that even minerals of relatively high radioactivity (several hundred to a few thousand ppm uranium) require exposure times of the order of ten days to yield a statistically significant number of countable  $\alpha$  tracks. It is very difficult to differentiate in a collection of  $\alpha$  tracks between those from the decay series of Th and those from the U decay series. It is also possible that there is not secular equilibrium in the U decay series. Therefore, unless through independent measurements the Th/U ratios of the radioactive minerals are known, or one assumes these ratios,  $\alpha$ -particle autoradiography does not furnish independent determinations of U and Th.

The fission track method, developed in the mid 1960's by Fleischer, Price, and Walker (1965) permits determination of the location and individual abundances of uranium, and under favourable conditions, thorium, in thin or polished sections after short exposures (generally a few minutes) to reactor neutrons. Over the past five years several workers have applied the method to study uranium contents, ranging usually from tens to hundreds of ppm, in thin and polished sections containing accessory and rock-forming minerals (for example, Kleeman and Lovering, 1967, Wollenberg and Smith, 1968). Uranium contents as low as a few tens of ppb have been measured in finely powdered preparations of whole-rock ultramafic samples (Fisher, 1970). Much less has been accomplished in the study of occurrences of thorium because of limitations of the method which will be discussed later in the text.

In this report I shall describe the physical background, technique, and results of determinations of U and Th in relatively high radioactivity minerals of the Ilímaussaq intrusion, South Greenland, and in a mineralized fault-zone occurrence in East Greenland. The purposes of the paper are to illustrate the usefulness of the fission-track method, and to present preliminary data on U and Th contents in mineralizations of possible future economic importance.

## 2. THE FISSION TRACK METHOD

Significant in the application of the fission phenomena to earth sciences are the facts that 1)  $^{232}\text{Th}$  and  $^{238}\text{U}$  fission readily under irradiation by fast neutrons, 2)  $^{235}\text{U}$  fissions most readily under thermal-neutron irradiation and, 3)  $^{238}\text{U}$  fissions spontaneously. ( $^{232}\text{Th}$ ,  $^{235}\text{U}$ , and  $^{234}\text{U}$  also fission spontaneously, but at much slower rates than  $^{238}\text{U}$ ). The energy threshold for fission of  $^{238}\text{U}$  and  $^{232}\text{Th}$  is 0.9 MeV; therefore, in rock samples thermal-neutron irradiation causes only  $^{235}\text{U}$  to fission. The spontaneous fission of  $^{238}\text{U}$ , though necessary for fission-track age determinations of a mineral, also yields a background of fission tracks in natural materials used as track detectors.

A fission track is formed when a massively charged fragment, emanating from a fissioned nucleus, enters the structure of a detector (generally a good insulating solid such as mica, plastic, or glass), causing damage by charge repulsion. The resulting damaged area is enhanced by etching the detector with the appropriate reagent: hydrofluoric acid (HF) for mica or glass, a strong base for plastic. One can then view the tracks or damage pits easily with an ordinary microscope.

The formation of tracks depends upon the specific ionization,  $\frac{dJ}{dx}$  (Fleischer et al., 1967), which determines the number of ions formed along the path of the fission fragment.  $\frac{dJ}{dx}$  is a function of the effective charge of the fragment, the fragment's velocity, the speed of light, the ionization energy of the outer electrons of the detecting material, the electron's mass, and a constant which depends on the detecting material.

For our purposes fragments from the fission of U or Th, with atomic mass numbers in the 90-140 range and average energies of 85 to 90 MeV, register nicely in muscovite mica, plastics, or glass. With proper etching conditions, tracks from the spontaneous fission of  $^{238}\text{U}$  have been observed in several rock-forming and accessory minerals.

The equation governing the density of fission tracks in a detector placed directly on the flat surface of material containing U, and irradiated with neutrons is:

$$\rho = \phi \sigma E n \quad (1)$$

where

$\rho$  is the track density in tracks/cm<sup>2</sup>,

$\phi$  is the integrated neutron flux, neutrons/cm<sup>2</sup>,

$\sigma$  is the neutron-induced fission cross section;  $\sim 580$  barns for thermal neutron fission of  $^{235}\text{U}$  (1 barn =  $10^{-24} \text{ cm}^2$ ),  
 $E$  the efficiency of detection (0.5 for our case), and  
 $n$  is the number of U nuclei per  $\text{cm}^2$  of thin section surface, within the effective range of fission fragments. For fragments from U and Th fission the effective range in most silicate and phosphate minerals is  $\sim 3 \text{ mg/cm}^2$ .

$$\text{Thus, } n = 3C/A, \quad (2)$$

where  $C$  is the concentration of radioelement in  $\text{g/g}$ ,

$a$  is Avogadro's number, and

$A$  is the atomic mass number of the radioelement.

In actual practice it is not necessary to use the above equations to determine element concentrations if standards are included in the neutron exposure. The equations are most useful in estimating the neutron flux required for an irradiation.

If uranium-free detectors are used, the lower limits of detection depend mainly on the magnitude of the integrated neutron flux (regulated in most cases by the duration of the exposure). For example, Fisher (1970) used an integrated flux of  $10^{16}$  neutrons/ $\text{cm}^2$  to measure U concentrations as low as a few ppb. The uranium content and geologic age of natural mica detectors combine to furnish a background track density which essentially governs their detection limit; 1 to 5 ppm with an integrated flux of  $\sim 10^{13}$  neutrons/ $\text{cm}^2$ . Therefore, such detectors are applicable to neutron-induced fission of U and Th in concentrations from several tens to thousands of ppm.

### 3. PROCEDURES

The basic procedure to obtain fission tracks from uranium and/or thorium is quite simple. Solid-state track detectors, usually mica or plastic, are mounted on a series of samples and standards, which are then exposed to reactor neutrons. On completion of the exposure the detectors are removed from samples and standards and etched in the appropriate reagents. The resulting tracks are then viewed and counted with the aid of a microscope. (A detailed scheme for obtaining fission tracks in muscovite and their observation, is given as Appendix 1).

### 3.1. Choice of Detectors

In choosing a fission track detector one must weigh the advantages and disadvantages of different materials. This discussion is limited to the two most commonly used in geologic applications, lexan polycarbonate plastic ("lexan" or "makrofol") and muscovite mica; they are compared briefly on table 1. Tracks in muscovite are long hexagons if etched for a short time, and develop into diamond shapes as etching progresses (fig. 1). Tracks appear in lexan as dark points (from fission fragments entering the detector perpendicular to the surface) or as dark lines whose apparent length depends upon the entry angle of the fragment and its starting position in the sample. Lexan's principal advantage is that it has essentially no background uranium content, while even the highest quality mica shows a background of tracks from spontaneous and induced fission of its  $^{238}\text{U}$  content. When examining minerals with U contents  $>10$  to 15 ppm, detector background is not a problem because track densities from the sample are considerably greater than background. If one expects low contents of U, he may prefer to use lexan detectors or expose a mica detector without sample to obtain the effective background value.

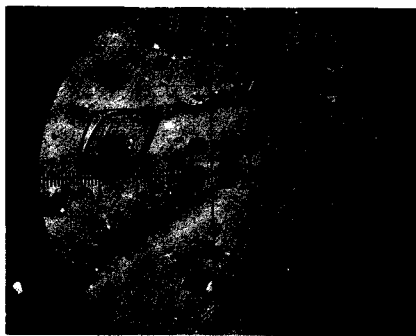


Fig. 1. Fission tracks in muscovite mica detector; large track, 16-hour etch, small tracks, 1.5-hour etch. Field diameter 0.27 mm.

Table 1

Comparison of Detector Materials

Natural Muscovite	Polycarbonate Plastic
Very durable	Surface scratches easily
Tracks easy to recognize, readily distinguished from scratches	Tracks perpendicular to surface appear as small dots, easily confused with scratches
Etching time 1/2 to 4 hours	Etching time 10 to 15 min
Track size regulated by varying etching time without danger of appreciable surface loss	Surface removed readily as etching progresses; not possible to enlarge tracks after 10 to 15 min
Uranium content plus geologic age yield background tracks from spontaneous and induced fission. This governs detection limit (1 to 5 ppm U)	Essentially no background tracks, detection limit governed by neutron exposure
	Print of rock surface forms after etching (Kleeman and Lovering, 1967)

### 3.2. Standards

To furnish track-density-element-content calibrations, and to serve as neutron flux monitors, glass standards containing known amounts of U and Th are irradiated along with the samples. The neutron flux may be depressed within a stack of thin-section-detector sandwiches; therefore, standard glasses inserted at the center and ends of the stack yield close approximations of the true calibration factors for each thin section. Soda disilicate ( $\text{Na}_2\text{O} \cdot 2\text{SiO}_2$ ) was used as the standard glass medium primarily because of its low melting temperature,  $\sim 1100^\circ$ . The range of fission fragments in glass is approximately the same as in most minerals.

### 3.3. Irradiation

The choice of irradiation conditions depends upon the element to be determined and its expected concentration. Easily observable track densities range from  $10^4$  to  $10^6$  tracks/cm<sup>2</sup>. To determine an appropriate thermal-neutron flux for a uranium irradiation, one combines desired track density with the samples' estimated U concentration in equations 1 and 2. The samples are exposed in the thermal column of the reactor (a position outside the core, surrounded by graphite to exclude fast neutrons), where the ratio thermal-to-fast neutrons is highest, preferably  $\geq 1000$ .

Conversely, a fast-neutron irradiation is used for thorium. Here the sample-detector package is placed as close as possible to the reactor's core, and is encased by at least a 3 mm thickness of cadmium to permit irradiation by as "pure" a flux of fast neutrons as possible. In the flux estimate for a thorium irradiation one must include the large contribution to the observed track density from  $^{238}\text{U}$ .

The estimated integrated neutron flux is then:

$$\varphi = \rho / E(\sigma_{\text{Th}} n_{\text{Th}} + \sigma_{\text{U}} n_{\text{U}}), \quad (3)$$

where  $\rho$  is the desired track density,

$\sigma_{\text{Th}}$  and  $\sigma_{\text{U}}$  are the fast neutron (neutron energy  $\sim 3$  MeV) fission cross sections for  $^{232}\text{Th}$  ( $\sim 0.3$  barn) and  $^{238}\text{U}$  ( $\sim 1.1$  barn) respectively, and  $n_{\text{Th}}$  and  $n_{\text{U}}$  are the estimated concentrations of Th and U nuclei.

### 3.4. Etching

Etching time is varied to achieve an optimum track size for a given track density. This is most important if tracks are counted from photo-

graphs of the detectors. In this respect mica has an advantage over lexan in that track size in mica can be controlled by HF etching time (see fig. 1), and very little of the mica's surface is removed, even while etching for several hours. After 10 to 15 minutes the strong base etchant used for lexan rapidly removes its surface, causing a continuous depletion of tracks with time; first the shallower tracks, then those of greater penetration.

### 3.5. Observation

To determine the location of the sites of radioelements, the detector with the developed tracks can be replaced on the thin section, or matching areas of sample and detector can be photographed separately and pictures compared (see detailed description in appendix). Associated track densities can be counted in the microscope, from photos, or if contrast and spacing permit, by machine, and in the case of a thermal-neutron exposure for U, are compared directly with the standard's track densities, giving the uranium content. Errors are from counting statistics accrued from measurements of the standards' and samples' track densities.

### 3.6. Thorium Determination

The use of fast neutrons permits a determination of Th content, if the Th/U ratio is great enough. Since practically all Th-bearing minerals also contain some U, it is necessary to first determine U by a thermal-neutron exposure. Then the sample, with a new detector and U and Th standards, is exposed to fast neutrons (energies  $> 1$  MeV, usually 3 to 4 MeV). The resulting track density is from  $^{238}\text{U}$  and  $^{232}\text{Th}$ , but knowing the U content, and having exposed a U standard along with the samples, the U contribution is determined. The contribution from Th is then the difference between the total track density and the contribution from U. The main difficulty with this method is that the relative errors due to counting statistics are rather large; the cross-section ratio for fast neutrons favours U over Th by a factor of  $\sim 3$ . Calculation of thorium and associated relative errors are discussed in section 4 of Appendix 1.

## **4. RESULTS AND DISCUSSION**

The fission track method has been applied to study the distribution of uranium and thorium in some minerals of the Ilfmaussaq alkaline intrusion, South Greenland, and the uranium mineralization of a fault zone in East Greenland. In both cases the results are of a preliminary nature; many

more observations covering a broader range of minerals and mineralizations are required before definite conclusions can be reached. The main purpose here is to present these data as an illustration of the usefulness of the fission track method, and through the discussion, to generate interest so that such studies are continued.

#### 4.1. Radioactive Minerals of the Ilímaussaq Intrusion

I first describe some results from examination of contents of radioelements in lujavrites and pegmatitic veins of Ilímaussaq. A location and geologic map of the intrusion is shown on fig. 2. In this stage of the study, the emphasis has been on the most ubiquitous radioactive minerals of the

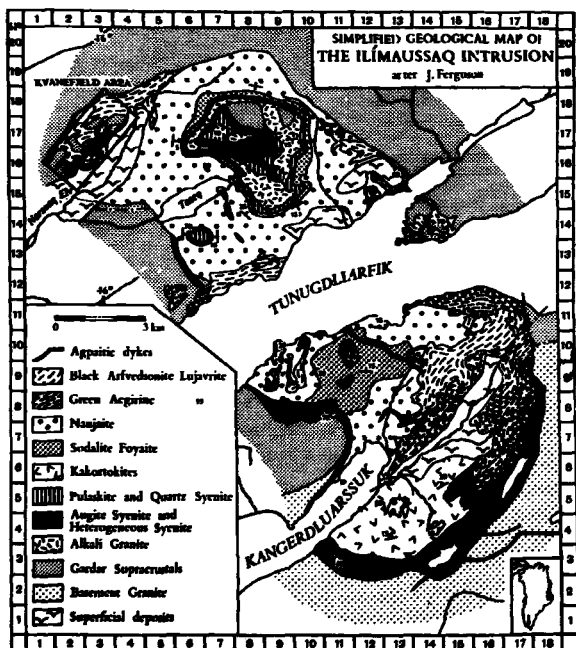


Fig. 2. Location and geologic map of the Ilímaussaq intrusion.



intrusion; steenstrupine, predominating in lujavrites of the Kvanefjeld area near the intrusion's northwest border (Sørensen et al., 1969), and eudialyte, which occurs in varying abundances (Ferguson, 1964, 1970, Hamilton, 1960, 1964), and appears to control whole-rock radioactivity in terranes outside of the Kvanefjeld area. Limited examinations have also been made on monazite, thorite and pigmentary material in Kvanefjeld lujavrite. Results of fission-track examinations of these Ilímaussaq minerals are listed on table 2. Professor Henning Sørensen describes the Ilímaussaq thin sections in Appendix 2.

#### 4.1.1. Steenstrupine

From examination of table 2, one can see that steenstrupine is characterized by a broad range of U and Th, even from grain to grain in a single thin section. An example is shown in samples from borehole 39 which was drilled in lujavrites of the Kvanefjeld. In rather homogeneous-appearing brown steenstrupine in the thin section from depth 156.60, U ranges from 2700 to 7000 ppm, Th from 13700 to 25700; approximately factor-of-two differences between nearly adjacent grains. However, there is fairly close agreement between the overall average Th/U (3.1) in steenstrupine of the borehole's thin sections with Th/U (2.7) of corresponding whole-rock samples. This substantiates the conclusion from observation of the thin sections that in this lujavrite, steenstrupine essentially controls whole-rock uranium and thorium. The ratios between whole-rock and steenstrupine Th and U contents indicate that steenstrupine makes up 2 to 4% of the rock.

The distribution of U and Th within a large steenstrupine grain from a pegmatite vein is illustrated graphically in fig. 3. The traverse shows a rather uniform distribution of uranium, while thorium varies over factors of two to three. The error bars associated with the thorium points are from counting statistics (discussed in the appendix).

Other steenstrupine grains were chosen for examination because of their marked zoning. One type of zoning is exemplified in reddish steenstrupine (described by Buchwald and Sørensen, 1961), sample 18467b-1. Here the centers of the grains appear somewhat isotropic under crossed nicol prisms, while the outer areas are anisotropic (fig. 4). Buchwald and Sørensen noted a marked difference in  $\alpha$ -particle activity of these grains; higher activities in the central portions, lower in the anisotropic borders. This is substantiated by the U and Th contents (table 2), which are approximately twice as high in the isotropic centers as in the border areas. Another type of zoning, edge-alteration of eudialyte, is illustrated in sample 66138. There is a

Table 2

Fission-track determination of U and Th in some minerals of the Khamovskoy intrusion

Sample Description	Uranium (ppm)			Thorium (ppm)			Whole Rock <sup>a</sup>			
	No. of meas.	Average	Range	No. of meas.	Average	Range	Th/U	U (ppm)	Th (ppm)	Th/U
Dioritopane in hornfels 20, in leucite of the Krasnfeld area										
2020, 05-10 "sandy" st.	6	5630	1180-13000	3	12400	1720-27700	2.2	364	700	1.9
2020, 8.03-08 pseudomorph after st.	5	6317	3300-14700	3	35033	3100-60000	4.3	412	1320	3.0
2020, 100 small st. crystals, clear to brown	7	8031	7730-10000	4	33000	17200-60000	3.6	330	723	2.5
2020, 145.57-57 sandy st.	7	7030	3415-8000	4	36100	12300-30000	2.4	270	330	2.0
2020, 150-60-60 brown st.	8	5630	2620-7000	3	17500	17700-25700	2.0	735	400	3.0
2020, 151.45-56 small st. crystals, brown and clear	5	5000	7705-12700	2	11000	7000-15000	1.2	115	300	2.5
Mean values for 2020		7530			22450		3.1	270	607	2.7
Other dioritopane mineralizations										
2715, small st.	2	2720	240, 3100							
2020, 21.01-10 small st. in leucite; radiolytic	4	1072	620-1710							
	2	71	56, 60							
2020, 55, 50 small subhedral st. grains	3	9213	3200-10000							
27-2, st. from pegmatite; mean values from traverse across large crystals	14	5000	5100-7630	14	43500	20000-70000	7.4			
20120 st. (?) rimming radiolytic rim zone; away from rim; radiolytic	3	6700	3100-8100							
	1	1200								
	2	410	200, 520							
100120 st.	2	4330	4300, 4000							
10467 b-1 small red st. isotropic zones; ultracrystalline borders	8	5450	4200-7200	1	33000		5.1			
	2	2355	1000, 2720	2	12650	7700, 20000	5.9			
10468 C-2 non-crystalline st.	2	2070	400, 3000							
71200 igneous material in mod. - one, arborescent leucite	4	18000	14000-25300	3	not detected ~ 3000					
Thorium (?) from this vein in arborescent-sugilite leucite	3	37000	20000, 35000	3	60.0%	20%, 50%	12.8			
Radiolytic in hornfels VII, in green leucite of the Krasnfeld area										
27.15-25	3	366	100-200					48		
2700-15	5	105	135-470	5	305	60 - 700	2.0	31	30	1.0
71.50	3	170	101-220					30		
62.10-20	3	100	105-265					36		
Mean values for VII		205						35.5		
Monazite in leucite of the Krasnfeld area										
With thorium (?) in this vein in arborescent-sugilite leucite	3	3300	3000, 3670	3	24.0%	10%, 30%	46.4			
71200	3	1220	540-2200	3	11800	6500-14000	8.7			
2020, 6.03-08	1	1010		1	12300		12.9			
2020, 140	3	2170	2050-2350	3	23200	10400-33600	11.7			

<sup>a</sup> Determined by T-spectrometric scans of 1-meter intervals of the core encompassing the thin-section locations.

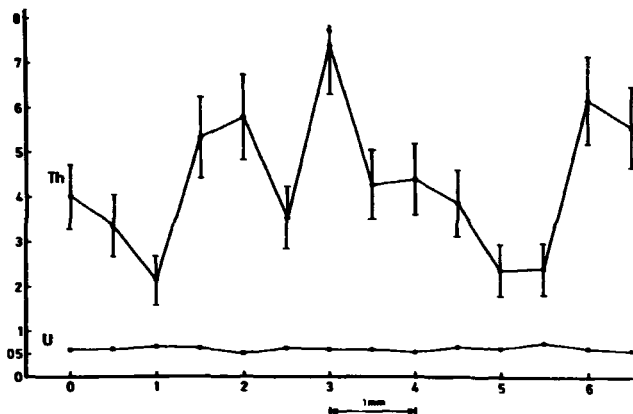


Fig. 3. Distribution of U and Th in profile across a large steenstrupine grain from a pegmatite.

sharp enrichment in uranium at the altered margin of a large crystal; the margin material may be steenstrupine. The U content drops off sharply from ~7000 ppm in the rim zone to 1000 to 1500 ppm in partially altered material, to ~400 ppm in apparently unaltered eudialyte (fig. 5).

The frequency distributions of U in all of the steenstrupine samples examined, and Th and Th/U in the borehole 39, red, and a pegmatitic steenstrupine, are shown on the histograms, fig. 6. As one might expect from the mineralizations described above, there are broad variations in Th and U within and between the various modes of occurrence of steenstrupine. Noteworthy are the broad ranges in borehole 39 steenstrupines from samplings over only a 160 meter interval of lujavrite.

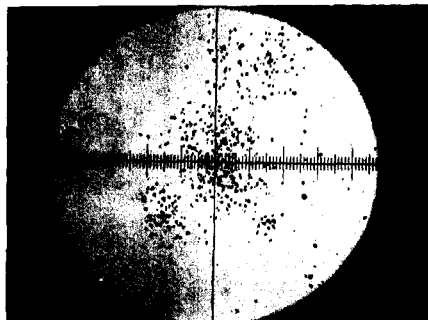
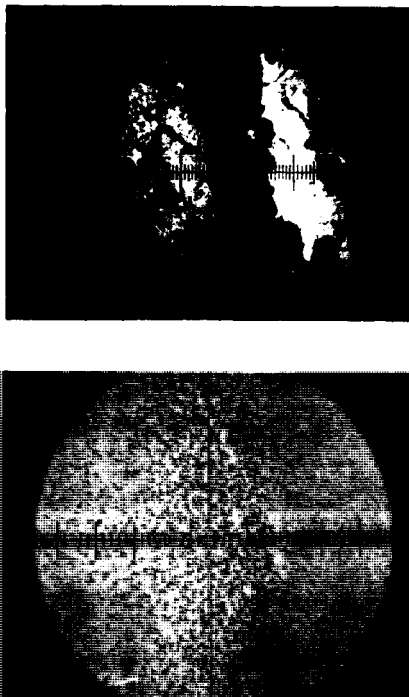


Fig. 4. Zoned reddish steenstrupine, showing fission tracks associated with U concentrated in the grain's isotropic center (4200 ppm), and a lower U content in the rim zone (2000 to 3000 ppm). Field diameter 1.2 mm.



**Fig. 5. Edge alteration of eudialyte in pegmatite, showing concentration of U in the rim zone (~ 7000 ppm) decreasing toward the interior of the crystal (400 ppm). Field diameter 1.2 mm.**

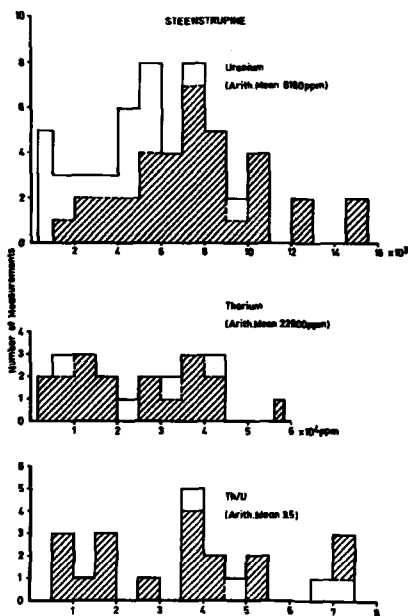


Fig. 6. Frequency distributions of U, Th, and Th/U in steenstrupine; lined areas represent steenstrupine from borehole 39.

#### 4.1.2. Eudialyte

There are large differences in the uranium content of eudialyte between different rock types. Uranium, averaging 209 ppm, appears rather evenly distributed in unaltered eudialyte from borehole VII (fig. 7, table 2), drilled in "green" (aegirine-arfvedsonite) lujavrite of the Kangerdluarssuk area in the southern portion of the Ilmaussaq intrusion. This contrasts with considerably lower U (50-100 ppm) in eudialyte closely associated with steenstrupine at 21 meters depth in borehole 43 of the Kvanefjeld. The borehole 43 eudialyte has a range of U similar to that reported by Hamilton (1964),

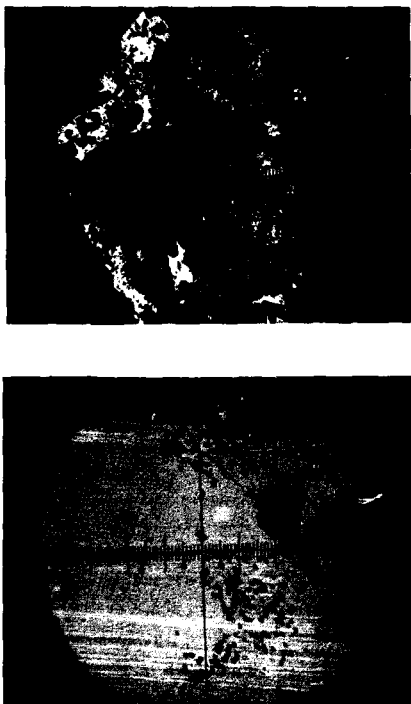


Fig. 7. Unaltered eudialyte in aegirine-arfvedsonite lujavrite, showing a rather even distribution of U (~200 ppm). Field diameter 1.2 mm.

60 ppm, in a sample from the northern portion of the intrusion. Higher uranium concentrations (300-500 ppm) were measured in the strongly zoned eudialyte of the aforementioned sample 76139. It appears that essentially all of the borehole VII lujavrite's radioactivity is controlled by U and Th in the eudialyte. The ratio of average U contents of eudialyte to average U in corresponding whole-rock samples is approximately 6, within the range, but somewhat lower than one might expect, given Ferguson's (1964) estimate of 10% eudialyte in green lujavrite.

#### 4.1.3. Pigmentary material

A cloudy, greenish-brown material has been observed between and coating arfvedsonite laths in fine- and medium- to coarse-grained lujavrite of the Kvanefjeld. It resembles somewhat Hansen's (1968) description of pigmentary material in radioactive veins. The pigmentary material, observed in sample 77290 (table 2 and fig. 8), contains up to 2.5% U with little or no thorium. This strong contribution solely from uranium, superimposed on those of Th and U in steenstrupine, may account for the relatively low whole-rock Th/U ratio, 1.54, observed in some arfvedsonite lujavrites of the Kvanefjeld (Løvborg et al., 1971). The apparent close association of pigmentary material with arfvedsonite, a mineral characterized by a predominance of  $\text{Fe}^{+2}$  over  $\text{Fe}^{+3}$ , may indicate reducing conditions favouring the selective localization of uranium.

#### 4.1.4. Thorite

Material considered likely to be thorite has been observed in veinlets of the Kvanefjeld (Løvborg et al., 1971). In thin section (fig. 9) it appears light yellowish-brown, and is associated with greenish cloudy monazite (see table 2). The high thorium (28 to 55%) and uranium contents (2 to 3%) of the thorite are consistent with those reported for the mineral in reference texts (see for example Nunninger, 1954).

#### 4.1.5. Monazite

This mineral, generally in cloudy-appearing aggregates of small elongate crystals (fig. 10), was examined in some drill cores and surface samples of lujavrite from the Kvanefjeld (table 2). Monazite associated with the thorite described above contains a large abundance, ~ 25%, of Th, and has a high Th/U ratio. Considerably lower Th contents, 1 to 2%, were measured in monazite from medium- to coarse-grained lujavrite of the Kvanefjeld; Th/U ratios in this monazite fall in the range 9 to 14. These are similar to the ratios in thorite, and contrast with the considerably lower Th/U measured in steenstrupine in the same thin sections.



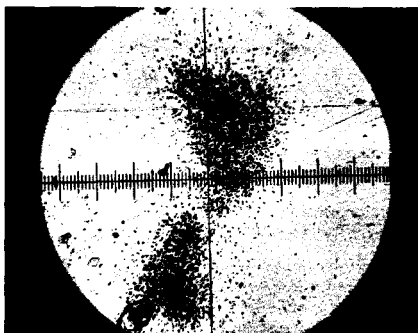
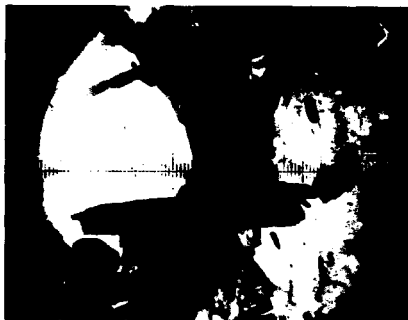


**Fig. 8. Pigmentary material (1.4 to 2.6% U) in and between grains of arvedsonite in lujavrite. Field diameter 1.2 mm.**



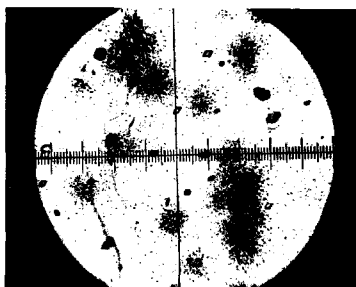


**Fig. 9.** Thorite (28 to 55% Th, 2 to 3% U) associated with greenish cloudy monazite in a violet in lujavrite. Field diameter 1,2 mm.





**Fig. 10. Fission tracks from U plus Th (U ~ 1200 ppm, Th ~ 12000 ppm) in monazite (gray) with arfvedsonite (black), in medium to coarse lujavrite. The large tracks are from a 16-hour etch prior to the fast-neutron exposure. Field diameter 1.2 mm.**

#### 4.2. Comparison with $\alpha$ -Autoradiographic Data

A comparison of uranium and thorium values with corresponding  $\alpha$ -track densities (table 3), reported by Buchwald and Sørensen (1961), indicates relatively good concurrence. Low  $\alpha$ -track densities of eudialyte from the green lujavrite of Kangerdluarssuk correspond to U ranging from 160 to 410 ppm. Considerably higher  $\alpha$ -track densities, varying over nearly a factor of 10 in steenstrupine of Kvanefjeld lujavrite, match broad ranges in U and Th in the borehole 39 series and in U in the samples from boreholes 43 and 35.

There is also good agreement between U and Th and  $\alpha$ -track data for isotropic and anisotropic zones in the red steenstrupine of sample 18467b-1. To directly compare Buchwald and Sørensen's observed  $\alpha$ -track densities with those calculated from fission track data, the mean U and Th values for the anisotropic and isotropic zones (table 3) were entered in the formula of Coppens (1952), which relates radioelement content with  $\alpha$ -track density. The resulting values, 8200 and 3500  $\alpha/\text{cm}^2$ -hour for isotropic and anisotropic zones respectively, fall within the reported  $\alpha$  density ranges.

Table 3

Comparison of  $\alpha$ -track data with radioelement contents

Description	$\alpha$ tracks/ $\text{cm}^2$ -hour <sup>a</sup>	U (ppm)	Th (ppm)
Steenstrupine in lujavrite, Kvanefjeld area	1300 to 12000	820 to 15000	1720 to 40000
Sample 18467b-1, zoned red Steenstrupine:			
anisotropic borders	3100 to 5300	2000 to 2700	7700 to 20000
isotropic centers	6200 to 8300	4200 to 7200	33000 (1 measurement)
Eudialyte in green lujavrite, Kangerdluarssuk area	100 to 640	210 <sup>b</sup>	

a) from Buchwald and Sørensen (1961)

b) mean value of borehole VII samples

### 4.3. An East Greenland Fault Zone Occurrence

The distribution of uranium in thin sections from a mineralized fault zone was investigated by the fission track method. The geology of the area has been described in general terms by Kempter (1961). The samples from which the thin sections were prepared consist of moderately to strongly oxidized fault breccia, mineralized with varying intensity, principally by fluorite and barite. Megascopic examinations coupled with Y-ray spectrometric determinations indicate that whole-rock uranium generally varies with the intensity of fluoritization.

Descriptions of uranium-rich material and associated U contents are given on table 4. It is apparent that U is closely, but in many cases, not directly associated with the fluorite; most generally U occurs with yellowish

Table 4

Uranium mineralizations at an East Greenland fault-zone occurrence.  
Fission track determinations of U in oxidized, brecciated vein material  
with quite varying amounts of fluorite and barite

Sample	Description	U (ppm)	Whole-rock <sup>b</sup> U (ppm)
1601	Transparent hexagonal grain (apatite?); (also observed anhedral translucent grain with very intense track density, several tens of % U)	2300	334
1618	"Pepper-like" fluoritized zone with abundant opaque grains	1800	691
1621	Limonitic material: Single reddish opaque grain:	950 1220 overall 2500 + on margins	2217
1624	Limonitic material inter-banded with and bordering a strongly fluoritized zone: Fl. zone without limonite:	2500 1600	446
2386	Translucent to opaque amorphous pigmentary mineralization containing at least several % U, superimposed on fluoritized zones of rather evenly distributed uranium; darker zone: lighter zone:	2000 to 2500 1050	88

<sup>b)</sup> Measured by Y-ray spectrometry of crushed-rock samples

to brownish limonite (?) which lines fluorite veinlets, is intergranular between fluorite grains, or exists separately from the veinlets (sample 1624, fig. 11). Uranium concentrations in this material range from several hundred to over 4000 ppm. Table 4 also describes some other less common associations of uranium, among which are a very intense (uncountable) fission track density, occurring with a translucent grain in sample 1601, and U enrichment at the margin of a single reddish semi-opaque grain (hematite?) in sample 1624 (fig. 12).

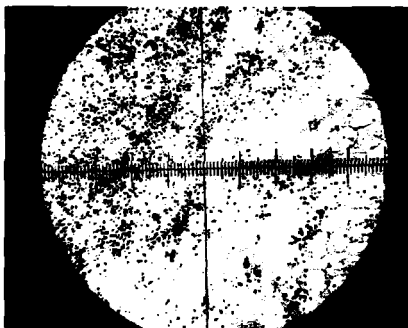
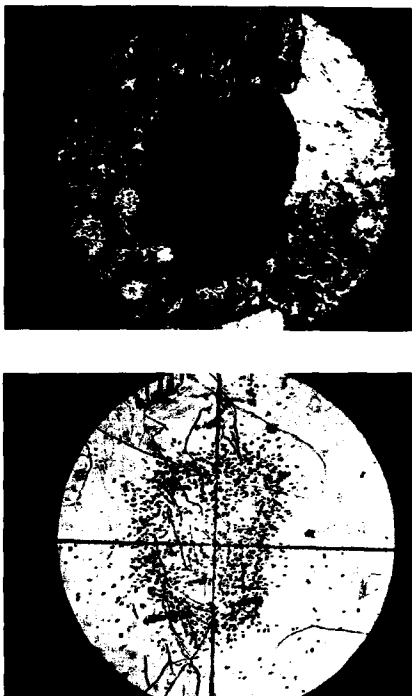


Fig. 11. Strong association of U (up to 4000 ppm) with limonite in fluoritised fault-zone breccia, East Greenland. Field diameter 1.2 mm.





**Fig. 12.** Enrichment in U (2500 to 3000 ppm) at the margin of an opaque grain (hematite ?) in fluoritized fault-zone breccia, East Greenland. Field diameter 0.88 mm.

Examination of table 4 indicates that there is little consistency between whole-rock uranium contents and those of the mineralized zones in the thin sections. In this occurrence uranium is confined to thin veinlets which are very unevenly distributed within the fault zone breccia.

## 5. SUMMARY AND CONCLUSIONS

The fission track method is a quick, simple, and inexpensive way to determine the location and abundance of uranium, and in some cases thorium, in uncovered thin sections. The method can be used to determine accurately U concentrations from several ppb up to several per cent. The accuracy for the determination of thorium is quite low when  $\text{Th/U} < 1$ , and improves to about 25% (relative error) with  $\text{Th/U} > 3$ .

In applying the method to the study of radioelements in the Ilímaussaq intrusion, it was observed that large disparities exist in the U and Th contents of steenstrupine grains only a few mm apart in lujavrite. This is reflected on a megascopic scale in field and laboratory  $\gamma$ -ray spectrometric measurements on lujavrites of the Kvanefjeld area (Løvborg et al., 1971). There is much less variation in uranium in the eudialyte of aegirine-arfvedsonite lujavrite in drill core from the Kangerdluarssuk area.

The fission track results and recent whole-rock  $\gamma$ -spectrometric measurements in the Ilímaussaq intrusion suggest strongly that steenstrupine governs whole-rock radioactivity in lujavrites of the Kvanefjeld area, while eudialyte controls radioactivity in lujavrites outside of the Kvanefjeld. The preponderance of eudialyte in kakortokite and naujaite, combined with their whole-rock uranium and thorium content (H. Wollenberg, unpublished data), indicate that eudialyte also governs the radioelement content of these rocks. X-ray fluorescence and  $\gamma$ -spectrometric data (Wollenberg et al., in press; Løvborg et al., 1971; and unpublished data) also show that there are characteristic ratios between contents of zirconium, lanthanum plus cerium, and radioelements in the rocks dominated by eudialyte, and in rocks where steenstrupine is most prevalent.

Like almost all geochemical techniques, the fission track method is most valuable when its results are combined with chemical data obtained by other methods. Directly applicable to the study of the Ilímaussaq minerals are electron microprobe examinations to disclose the composition of the lujavrites' pigmentary material, and similar examinations of the zoned steenstrupine and eudialyte. Though uranium is most commonly associated with fluorite and limonite in the East Greenland fault zone occurrence, there are occasional high concentrations in other unidentified minerals. As with the Ilímaussaq minerals, microprobe analyses may indicate the composition of these uranium-rich grains. The uranium and thorium balance in a rock unit may be obtained by combining data from whole-rock  $\gamma$ -spectrometric analyses with fission track measurements on populations of separated mineral grains.

## 6. ACKNOWLEDGEMENTS

I wish to thank Professor Henning Sørensen and John Rose-Hansen of the Institute of Petrology, Copenhagen University, for providing the thin sections upon which this work is based. Professor Sørensen offered valuable suggestions on the manuscript and furnished a description of the thin sections, included as Appendix 2. Preben Nielsen of Risø's photographic laboratory gave assistance in thin-section and track photography. Support of the fission track studies by my colleague, Leif Løvborg, and Jens Rasmussen, leader of the Risø Electronics Department, is gratefully acknowledged.

## 7. APPENDIX 1

A scheme for preparation, exposure and observation of a thin section-track detector series:

In this discussion we consider an exposure of thin sections with mica detectors<sup>a)</sup> to thermal neutrons in the thermal column of Risø's DR 2 reactor, and subsequent determination of uranium content.

### 1. Preparation

Clean micas in acetone, dry, mount with tape on uncovered thin sections and standards, record orientation by use of marks on the mica (for example, clip two opposite corners) so that the detectors can occupy the same position on the thin sections after etching. Standards with detectors are placed at each end and in the center of the assembled package. Measure and record position of each thin section and standard in the package.

### 2. Exposure

Table 5 lists exposure, processing, and observation conditions for various uranium contents. For U determination use the thermal column of the reactor, a position surrounded by graphite so that essentially only thermal neutrons are present (only  $^{235}\text{U}$  fissions). For example, in Risø's DR 2 reactor the position in the thermal column farthest from the reactor's core has a ratio

$$\frac{\text{thermal neutrons}}{\text{fast neutrons}} \sim 1000.$$

At this position the usual neutron flux is  $\sim 1.3 \times 10^{11} \frac{\text{neutrons}}{\text{cm}^2 \cdot \text{sec}}$ . Upon removal of the samples from the reactor allow a few days' cooling period for decay of short- and medium-lived induced  $\gamma$  radioactivity. The amount of activity depends on the length of exposure; generally  $\text{Na}^{24}$  (15 hr half life) is the predominant  $\gamma$  activity.

---

a) A good detector, "clear ruby mica" is obtained from the Micanite and Inculators Co. Ltd., Empire Works, Walthamstow, London E17; in Denmark through Carl Brinker Elektrotekniske Halvfabrikata, Skyttegade 7, 2200 København N. The cost is  $\sim 0.50 \text{ Dkr./cm}^2$ , plus moms.

Table 5

Exposure, processing, and observation conditions for various uranium concentrations

U content (ppm)	neutron exposure (n/cm <sup>2</sup> )	track density (t/cm <sup>2</sup> )	etching time <sup>a</sup> (hours)	magnification	tracks/field
50	$2 \times 10^{13}$	$1.2 \times 10^4$	3 to 4	x 36	~ 500
500	$1 \times 10^{13}$	$6 \times 10^4$	2 to 3	x 80	~ 450
5000	$1 \times 10^{13}$	$6 \times 10^5$	1 to 2	x 270	~ 400

a) Etching of high-quality muscovite mica in 40 to 48% HF at room temperature.

### 3. Processing

Remove micas from the thin section, clean in acetone, and place in 40 to 48% HF at room temperature for 1 to 4 hours, depending on the size of tracks desired. If one expects a low track density ( $\sim 10^3$  to  $10^4$  tracks/cm<sup>2</sup>) allow etching for a long period, perhaps 3 to 4 hours, to develop large tracks which can be counted under low magnification. If one expects a high track density ( $5 \times 10^4$  to  $10^6$  t/cm<sup>2</sup> or greater) etch for about 1 hour, then observe tracks to be certain that they do not become so large that they over-coalesce. (Polycarbonate plastic is etched in 5 to 6 N NaOH or KOH at 60° C for about 15 min.) On removal from the HF, wash the mica in water and dry. It is ready for observation.

### 4. Observation

To determine the calibration constants, first determine the track density of the micas from the standards. There will probably be a difference in track density between standards from the ends and center of the package (usually not greater than a factor of 1.5) due to neutron flux depression by a thick package and perturbations in the external flux at this distance from the reactor's core. A graph relating this difference to the position of the thin sections in the package is constructed, furnishing a close approximation to the true calibration factor (in tracks per cm<sup>2</sup> per ppm U) for each example.

The orientation of a mica-thin-section sandwich for exposure and observation is shown on fig. 13. For observation, the mica is taped to a clean glass slide with etched side up. The thin section with rock surface down is placed on the mica, so that a mineral of interest is viewed through the thin section's glass. A polaroid photograph can be made of the mineral, the thin section removed, and the associated cluster of tracks observed and photographed. Low magnification is used for location of minerals of high U-Th

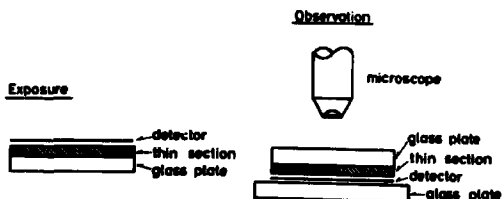


Fig. 13. Orientation of a detector-thin section sandwich for exposure and observation.

content, then tracks are counted under high magnification (see table 5), and the resulting track density compared with the calibration factor for the thin section, yielding the U content.

Mica detectors exposed to a fast neutron flux for fission of  $^{238}\text{U}$  and  $^{232}\text{Th}$  are prepared and etched in the manner described for  $^{235}\text{U}$ . One must note that thorium standards usually also contain some U; standards made from New Brunswick Laboratory 1% Th powder have a U/Th ratio of  $\sim 0.04$ . This must be taken into account when calculating the thorium calibration factor from the Th standards' track densities. The inherent uranium's contribution to the Th standards' observed track density is calculated from the calibration data of pure uranium standards, exposed concurrently.

After etching, the mica detectors from the samples are mounted on clear glass slides with the same orientation as the micas from the previous  $^{235}\text{U}$  exposure. The two detectors for each sample are then superimposed under the microscope, a track density from a given location counted first on one detector, then on the other. The location's U content is determined as described above.

The thorium content for the locations is then:

$$C_{\text{Th}} = (\rho_{\text{tot}} - (\text{Cu} \cdot \text{Calu})) / \text{Calth},$$

where

$\rho_{\text{tot}}$  is the observed track density from the fast neutron exposure,  
 Cu is the predetermined U concentration,  
 Calu is the U calibration factor from the fast neutron exposure, and  
 Calth is the thorium calibration factor from the fast neutron exposure.

The error in the thorium determination results from the accumulation of counting statistics in measurements of U and Th standards, and the samples' track densities from fast- and thermal-neutron exposures. Fig. 14 relates the samples' Th/U ratios and relative errors in Th for typical exposure and counting conditions of grains of steenstrupine and pigmentary material. Relative errors are less than 25% if Th/U is greater than  $\sim 3$ ; for ratios less than 3 the errors increase rapidly, and are considered unacceptably high ( $> 40\%$ ) for Th/U less than 1.

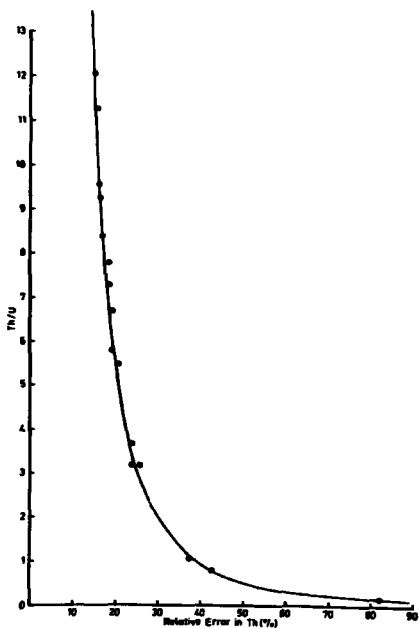


Fig. 14. Th/U ratio versus relative error in Th for typical exposure and counting conditions.



## 8. APPENDIX 2

### Description of Some of the Examined Ilímaussaq Thin Sections

#### I. Drill hole 39

0.05-0.10 m: Green fine- to medium-grained lujavrite. Weakly developed igneous lamination due to the parallel arrangement of irregular laths of microcline and irregular prisms of aegirine-acmite. The matrix consists of analcime which has corroded the microcline and aegirine. Nepheline is a minor component.

There are scattered small crystals of monazite and larger aggregates of monazite. Irregularly shaped dusty areas may be pseudomorphs after steenstrupine. They have patches of brown weakly anisotropic steenstrupine and also contain monazite.

There are small grains of an opaque mineral.

6.83-6.88 m: Green medium- to coarse-grained lujavrite with intergranular texture due to the arrangement of large laths of microcline. The interstitial areas are occupied by prisms of aegirine-acmite, partly forming aggregates, aggregates of small laths of microcline, analcime and aggregates of fine-grained natrolite. Analcime and natrolite crowded with flakes of white mica may substitute for nepheline.

There are large aggregates of dark-coloured monazite. Some of these aggregates are extremely fine-grained; others fairly coarse. Some aggregates display crystal outlines and as they contain patches of steenstrupine they may be secondary after this mineral. There are also apatite-appearing grains and patches rich in catapleiite.

The aegirine-acmite prisms contain inclusions of fluorite, steenstrupine and pseudomorphs after eudialyte.

The groundmass also contains catapleiite-rich pseudomorphs after eudialyte which may have rims of steenstrupine.

Cavities in the microcline have minute flakes of a white mica (Li-mica?). Sphalerite is a minor component.

140 m: Black laminated arfvedsonite lujavrite with scattered villiaumite and with acmite-rich patches.

The arfvedsonite lujavrite is composed of thin laths of albite, arfvedsonite, nepheline, sodalite, a little acmite, and subordinate amounts of the "green mineral" (unidentified Na-RE-P-mineral). There are numerous small crystals of steenstrupine, which are colourless to brown, and also

aggregates of monazite. Minor components are sphalerite and lovozerite. There are areas rich in analcime and microcline.

The acmite-rich patches have, in addition to the above-mentioned minerals, ussingite and lovozerite, and are rich in steenstrupine, the "green mineral" and nepheline. These patches appear to be associated with veins of sodalite-nepheline urtite with matrix of analcime.

145.51-145.57 m: Laminated arfvedsonite lujavrite rich in villiaumite and of a somewhat mottled appearance with darker and lighter-coloured "schlieren".

The arfvedsonite lujavrite is composed of albite, microcline, nepheline, sodalite and arfvedsonite. There are small needles of aegirine, small crystals of lovozerite and numerous crystals of steenstrupine, often in clusters made up of several crystals. These concentrations of steenstrupine are especially found in dark arfvedsonite-rich schlieren.

There are scattered grains of the "green mineral".

Light-coloured schlieren and patches have ussingite and acmite.

156.60-156.69 m: Laminated arfvedsonite lujavrite with many mm-sized holes.

In a matrix of analcime there are laths of albite and microcline and prismatic grains of arfvedsonite, all in parallel orientation. Also observed are corroded grains of nepheline and sodalite. There are numerous small crystals of steenstrupine, either clear or brown and minor acmite, mica, sphalerite, pectolite, the "green mineral" and epistolite (?). The "green mineral" is partly substituted by monazite.

157.47-157.56 m: Light-coloured arfvedsonite lujavrite with "layers" of green aegirine lujavrite.

The light-coloured rock is dominated by parallel laths of albite and microcline. The remaining minerals are nepheline, sodalite, analcime, arfvedsonite, aegirine and crystals of steenstrupine. There are scattered grains of the "green mineral", and aggregates of eudialyte crystals. The eudialyte crystals are partly poikilitic with inclusions, mainly of aegirine. The eudialyte is not of the usual appearance in thin section. It may wrap crystals of brown steenstrupine. There are aggregates of fine-grained monazite.

## II. Other samples

Drill hole 43, 23.01-23.06 m, Kvanefjeld: Eudialyte-rich pegmatite in

naujaite. The eudialyte crystals are surrounded by yellowish zones of alteration, which are up to 5 mm wide.

Under the microscope the eudialyte crystals are seen to be shattered with aegirine-acmite, arfvedsonite, pectolite, sodalite and minor neptunite and microcline filling the fissures.

The marginal alteration zones are composed of a pigmentary, optically isotropic material which should most probably be termed zirfecite. Steenstrupine has not been observed with certainty but brownish parts of the alteration zones have resemblance to steenstrupine. There are also turbid patches, which are weakly birefringent and which appear to be altered lovozerite. These alteration products penetrate into the eudialyte along fissures. Catapleiite has not been observed.

No. 66139: Pegmatite in naujaite, the head of the Kangerdluarssuq fjord. Large crystals of eudialyte have thin brown rims. The altered eudialyte is in contact with a replacement body of albite, natrolite, analcime, aegirine, pectolite and steenstrupine.

The eudialyte crystals have fracture-fillings made up mainly of aegirine and microcline.

The brown coatings are seen to branch as a fine network a short distance into the crystals. The alteration zones are anisotropic and optically continuous with the unaltered eudialyte. They are first of all distinguished by rust-filled fractures and by dots of brownish pigmentation. Large brown areas resemble steenstrupine and are optically isotropic.

Drill hole 35, 59.50 m, Kvanefjeld: Steenstrupine-arfvedsonite lujavrite.

There are bands rich in albite laths and bands having a matrix of analcime. The former are rich in arfvedsonite, the latter in acmite. Nepheline and natrolite are minor components.

The steenstrupine crystals are brown, often with darker cores and margins which are optically isotropic and an intermediate clear brown zone which is anisotropic.

No. 18467 b-1. Aegirine-steenstrupine vein in naujaite: The head of Kangerdluarssuq.

Aggregates of small steenstrupine crystals are enclosed in schlieren of felt-like aegirine and in intervening masses of analcime with small needles of arfvedsonite.

The steenstrupine crystals are zoned having dark, optically isotropic cores, and clear brownish-coloured marginal zones which are anisotropic. There may be thin isotropic zones parallel to the crystal faces in the

anisotropic marginal parts of the crystals. There is generally a faintly stronger brown colouration in a thin surface film and along marginal cracks.

No. 18491 e. Albitite vein in naujaite: Tugtup agtakorfia.

Steenstrupine crystals, up to one cm across, occur in a matrix of albite and microcline together with crystals of pectolite, Li-mica, acmite, sphalerite and epistolite. There are inclusions of arfvedsonite in the acmite.

The steenstrupine crystals are colourless to brown in thin section, distinctly birefringent and often zoned with dark-coloured cores.

Monazite-thorite-analcime-veins. Kvanefjeld: In a matrix of analcime there is an intergranular network and larger patches made up of aggregates of spindle-shaped monazite and anhedral "thorite" in a matrix of analcime. The aggregates also have arfvedsonite, neptunite, schizolite, steenstrupine, and pseudomorphs after "lovozerite".

The monazite is dark brown, and strongly pigmentated. The thorite is yellow, clear and optically isotropic. The steenstrupine is yellowish to brown and sometimes anisotropic.

In the analcime matrix there are small pseudomorphs after lovozerite (?).

## 9. REFERENCES

- Bowie, S.H.U., 1954, Nuclear Emulsion Techniques. In: Nuclear Geology, Edited by Henry Faul (Wiley, New York) 414 pp.
- Buchwald, V. and H. Sørensen, 1961. Autoradiographic Examination of Rocks and Minerals from the Ilfmaussaq Batholith, S.W. Greenland, Grønlands Geol. Surv. Bull. No. 28, also Medd. Grønland, 162, No. 11.
- Coppens, R., 1952 Etude de la radioactivite de quelques roches par emulsion photographie, Bull. Soc. Fr. Mineral. Cristallogr. 75, 57-58.
- Fleischer, R. L., P. B. Price, and R. M. Walker, 1965, Tracks of Charged Particles in Solids, Science, 149, 383-393.
- Fleischer, R. L., P. B. Price, R. M. Walker, and E. L. Hubbard, 1967, Criterion for Registration in Dielectric Track Detectors, Phys. Rev., 156, 353-55.
- Ferguson, J., 1964, Geology of the Ilfmaussaq Alkaline Intrusion, South Greenland, Grønlands Geol. Surv. Bull. No. 39, also Medd. Grønland, 172, No. 4.
- Ferguson, J., 1970, The Significance of the Kakortokite in the Evolution of the Ilfmaussaq Intrusion, South Greenland, Grønlands Geol. Surv. Bull. No. 89, also Medd. Grønland, 190, No. 1.
- Fisher, D. E., 1970, Homogenized Fission Track Determination of Uranium in Whole-Rock Geologic Samples, Anal. Chem. 42, 414-16.
- Hamilton, E., 1960, The Distribution of Radioactivity in the Major Rock-forming Minerals, Grønlands Geol. Surv. Misc. Papers No. 26, also Medd. Grønland 162, No. 8.
- Hamilton, E., 1964, The Geochemistry of the Northern Part of the Ilfmaussaq Intrusion, S.W. Greenland, Bull. Grønlands Geol. Surv. No. 42, also Medd. Grønland, 162, No. 10.
- Hansen, J., 1968, A Study of Radioactive Veins Containing Rare-Earth Minerals in the Area Surrounding the Ilfmaussaq Alkaline Intrusion, South Greenland, Grønlands Geol. Surv. Bull. No. 76, also Medd. Grønland, 181, No. 8.
- Kempton, Enrico, 1961, Die Jungpaläozoischen Sedimente von Süd Scoresby Land, Medd. Grønland, 164, No. 1.

- Kleeman, J. D. and J. F. Lovering, 1967, Uranium Distribution in Rocks by Fission-Track Registration in Lexan Plastic, *Science*, 156, 512-13.
- Kleeman, J. D., and J. F. Lovering, 1970, Lexan Plastic Prints; How Are They Formed?, *Radiat. Eff.* 5, 21-26.
- Løvborg, L., H. Wollenberg, P. Sørensen, and J. Hansen, 1971, Field Determination of U and Th by Gamma-Ray Spectrometry, Exemplified by Measurements in the Ilímaussaq Alkaline Intrusion, South Greenland, *Econ. Geol.*, 66, 368-84.
- Nininger, R. D., 1954, *Minerals for Atomic Energy* (Van Nostrand, New York) 367 pp.
- Sørensen, H., J. Hansen, and E. Bondesen, 1969, Preliminary Account of the Geology of the Kvanefjeld Area of the Ilímaussaq Intrusion, South Greenland, *Grønlands Geol. Surv.*, Rept. No. 18.
- Wollenberg, H. A., and A. R. Smith, 1968, Radiogeologic Studies in the Central Part of the Sierra Nevada Batholith, California, *J. Geophys. Res.*, 73, 1481-95.
- Wollenberg, H. A., H. Kunzendorf, and J. Rose-Hansen, 1971, Isotope-excited X-Ray Fluorescence Analyses for Nb, Zr, and La plus Ce on Outcrops in the Ilímaussaq Intrusion, South Greenland, *Econ. Geol.* (in press).